Ocean Sci. Discuss., 8, 1979–1999, 2011
www.ocean-sci-discuss.net/8/1979/2011/
doi:10.5194/osd-8-1979-2011

Ocean Science Discussions

Net primary productivity, upwelling and coastal currents in the Gulf of Ulloa, Baja California, Mexico

E. González-Rodríguez[1], A. Trasviña-Castro[2], G. Gaxiola-Castro[3], L. Zamudio[4], and R. Cervantes-Duarte[5]

[1]Centro de Investigación Científica y de Educación Superior de Ensenada (CICESE), Unidad La Paz, Miraflores No. 334, Fracc. Bella Vista, La Paz BCS, 23050, Mexico
[2]CICESE, Unidad La Paz Physical Oceanography Department, Mexico
[3]CICESE, Biological Oceanography Department. Ensenada, BC, Mexico
[4]Center for Ocean and Atmospheric Prediction Studies. Florida State University, Tallahassee, FL 32306, USA
[5]Centro Interdisciplinario de Ciencias Marinas (CICIMAR-IPN), Oceanology Department La Paz, BCS, Mexico

Received: 26 August 2011 – Accepted: 7 September 2011 – Published: 27 September 2011

Correspondence to: E. González-Rodríguez (egonzale@cicese.mx)

Published by Copernicus Publications on behalf of the European Geosciences Union.

Abstract

The Gulf of Ulloa, a highly productive area off the western coast of Baja California Peninsula, is examined for five successive years (2003–2007) by using satellite data and seasonal net primary productivity estimates obtained by a vertical generalized production model. The results clearly identify a seasonal signal of coastal upwelling in productivity estimates. Highest values occur from May to June and sometimes July. We also find influence of an equatorward coastal current able of transporting water from neighboring north upwelling areas to the Gulf of Ulloa in winter–spring. This flow contributes to increase the seasonal net primary productivity. The opposite occurs in summer, when a warm poleward current of tropical characteristics arrives to the region. Our findings reveal that such warm coastal current suppressed the productivity in the whole.

1 Introduction

The Gulf of Ulloa (Fig. 1) is the shallow sea off the west coast of the Baja California Peninsula limited to the north by Punta Eugenia (28° N 115°30′ W) and to the south by Bahía Magdalena (25° N 111°30′ W). The shelf is about 20 km wide off Bahía Magdalena, it widens to about 100 km in the central part of the Gulf and it narrows and almost disappears in the north, near Punta Eugenia. Historically the Gulf of Ulloa has been associated to high levels of biological productivity and for this reason is considerate as a Biological Activity Center (Lluch-Belda, 1999).

The west coast of the Baja California Peninsula belongs to the oceanographic region of the California Current System (CCS) and the region of interest is on its southern boundary. The California Current (CC) meanders offshore and modifies coastal hydrographic properties when it approaches the coast. Its surface expression is more intense in May–June when the CC forms the weak Cabo San Lucas front, a boundary between the subartic and subtropical waters off the entrance to the Gulf of California.

OSD
8, 1979–1999, 2011

A description of the CC can be found in the keynote papers of Hickey (1979) and Lynn and Simpson (1987). The whole CC region is characterized by the presence of meanders, eddies and a coastal transition zone (CTZ) between it and the coastal waters during upwelling season. This CTZ contains large filaments and eddies that contribute to the offshore transport of properties (Brink and Cowles, 1991). The western shelf is part of the active geological features of the peninsula, so it is actually formed by intense bathymetric gradients. As a result, the shelf width varies from a narrow coastal shelf with steep gradient to gentle slopes of substantial width (Zaytsev et al., 2003).

The shelf of the western Baja California Peninsula has been considered highly productivity, especially on the coastal upwelling regions (Lluch-Belda, 1999; Zaytsev et al., 2003). This coastal upwelling process is developed when equatorward winds blow over the oceans surface creating a stress that gives the ocean a horizontal initial velocity in the direction of the wind, but the Coriolis Effect due to the Earth's rotation exerts acceleration proportional to velocity at right angles to the direction of motion, this turns the ocean velocity away from the direction of the wind, and the resulting Ekman transport is 90°. When the Ekman transport is horizontally divergent, a vertical transport, called Ekman pumping, into the boundary layer is created.

Upwelling regions in the CCS are been located from Cabo Mendocino to Pt. Conception in California and along coast most of Baja California Peninsula (Nelson, 1977; Bakun and Nelson, 1977; Huyer, 1983). Specifically in the Gulf of Ulloa, from April to July (Lynn, 1967) found the presence of narrow coastal cold water south of Punta Eugenia. The shape of the coastline is an important factor determining the location of upwelling centers as well as the generation of eddies and filaments (Haynes et al., 1993). Along the entire coast of the Baja California Peninsula the upwelling intensity changes in accordance with local wind conditions and bottom topography. Zaytsev et al. (2003) identified the seasonal and latitudinal variability of upwelling processes and found that the most permanent upwelling zones south of 28° N are located off Bahía Tortugas and off Bahía Magdalena (North and South of the Gulf of Ulloa, respectively).

OSD
8, 1979–1999, 2011

In this report the effect of upwelling and coastal currents over the net primary productivity (NPP) off the west coast of Southern Baja California is described. To determine if a relationship exists between NPP, advection due to coastal currents and the Ekman pumping produced during upwellings, we use monthly imagery of satellite sea surface temperature, geostrophic currents estimated from altimetry data and wind stress curl estimated from Quikscat satellite products.

2 Methods

To characterize the seasonal behavior of NPP in the Gulf of Ulloa we use monthly maps of NPP from a vertical generalized productivity model (VGPM) for the period 2003–2007 between 24° to 29° N and from 116° to 111° W. The VGPM used to estimate the net primary productivity (NPP) is the model proposed by Behrenfeld and Falkowski (1997), based on the following equation

$$\mathrm{NPP} = f_{\mathrm{PAR}} \cdot \mathrm{Cl}\text{-}a \cdot \mathrm{Pb} \cdot D_{\mathrm{irr}} \cdot Z_{\mathrm{eu}} \quad (1)$$

Where:

- NPP is the net primary productivity in mg C $\mathrm{m}^{-2}\,\mathrm{d}^{-1}$.
- f_{PAR} is the Photosynthetically Active Radiation in Einstein $\mathrm{m}^{-2}\,\mathrm{d}^{-1}$. Obtained from SEAWIFS satellite.
- Cl-*a* is the satellite surface chlorophyll-*a* concentration in mg m^{-3}. Obtained from MODIS satellite.
- Pb is also known as $\mathrm{Pb}_{\mathrm{opt}}$ and it is the maximum rate of carbon fixation in the water column in mg C mg Cl-$a^{-1}\,\mathrm{h}^{-1}$. $\mathrm{Pb}_{\mathrm{opt}}$ was derived from satellite SST (MODIS) by fitting a polynomial to a large number of field $\mathrm{Pb}_{\mathrm{opt}}$ values (Behrenfeld and Falkowski, 1997).

OSD
8, 1979–1999, 2011

– D_{irr} are the daily hours of light. A Matlab function to get the D_{irr} was created according to http://www.science.oregonstate.edu/ocean.productivity/vgpm.model.php.

– Z_{eu} is the euphotic zone depth in m. For this study, the euphotic zone depth was substituted by the mixed layer depths (MLD) obtained from results of the high resolution ocean general circulation model, HYCOM (Bleck, 2002), so the final model was rewritten as follows:

$$\mathrm{NPP} = f_{\mathrm{PAR}} \cdot \mathrm{Cl}\text{-}a \cdot \mathrm{Pb} \cdot D_{\mathrm{irr}} \cdot \mathrm{MLD} \quad (2)$$

All variables, except D_{irr} and MLD were obtained from satellite monthly data at 4 × 4 km of resolution (Level 3, http://oceancolor.gsfc.nasa.gov/cgi/l3). The daily D_{irr} and MLD were recalculated to feed the monthly model time scale (the model is written in the MATLAB programming language).

The MLD was used because it is not influenced by the particle content, as happens with the euphotic zone depth (Z_{eu}) during the coastal upwelling. The (Z_{eu}) was calculated using the Morel and Berthon (1989) case I model, which estimates (Z_{eu}) from surface chlorophyll concentrations. We tested this hypothesis by comparing both variables using Z_{eu} from MODIS imagery with MLD from HYCOM. A linear relationship between Z_{eu} and MLD was found during the upwelling months (March to June). Figure 2a and 2b shows an example of such relationship for a typical spring with a slope close to 1 (0.88 and 1.28, respectively).

Monthly maps of satellite sea surface temperature (SST) were also generated with data from MODIS-AQUA level 3 at 4 × 4 km of spatial resolution available from ocean color home page, http://oceancolor.gsfc.nasa.gov, which is a dimensional array of the globe in an equidistant cylindrical projection stored in HDF format file. The algorithm chosen for SST was the one which use the daytime (11 µm) data.

Monthly maps of satellite geostrophic currents (designated as "currents" in the rest of the paper) were estimated from altimetry data following the method described in

OSD
8, 1979–1999, 2011

Strub and James (2002). Sea level heights are obtained by adding the sea level anomaly from the satellite to the mean sea level long-term climatology from Levitus and Gelfeld (1992). The altimeter *msla* (map sea level anomalies) products are produced by Ssalto/Duacs and distributed by AVISO (http://www.aviso.oceanobs.com/en/data/products/sea-surface-height-products/global/msla/index.html). The maps resolve the current field in a horizontal grid of one-third of a degree.

Monthly maps of wind and wind stress curl (WSC, proportional to the vertical upwelling velocity produced by Ekman pumping), were derived from daily averaged QUIKSCAT wind data (http://winds.jpl.nasa.gov/missions/quikscat/index.cfm). This is based on the following equation (Gill, 1982),

$$\mathrm{WSC} = \frac{1}{pf}\left\{\frac{\partial Y_\mathrm{s}}{\partial x} - \frac{\partial X_\mathrm{s}}{\partial y}\right\} \tag{3}$$

where:
X_s and Y_s are the wind stress components
p is the density of water
f is the Coriolis parameter

The wind stress curl (WSC) is an "index" of upwelling intensity since the vertical ("pumping") velocity is proportional to it (Gill, 1982). Positive/negative curl causes divergence/convergence in the Ekman layer and upward/downward Ekman pumping.

Climatological monthly maps for the period (2003–2007) and for all variables (NPP, SST, winds, WSC and currents) were generated averaging the monthly maps previously created. Next, to determine the seasonal behavior of the NPP, geostrophic currents and WSC during the whole period (2003–2007) monthly time series were generated at the 6 points marked in Fig. 1 (along the continental slope). Here we discuss the average of these time series. In the case of the time series of currents only the alongshore component ($V \cdot g$) is considered. This is the result of rotating the reference frame to have alongshore and cross-shelf currents. Positive/negative values of

OSD
8, 1979–1999, 2011

the alongshore component indicate a poleward/equatorward current. We call this the geostrophic alongshore current (GAC).

A harmonic analysis of the last three time series (NPP, GAC and WSC) was carried out. We used the method of periodic regression (Bliss, 1958) to find the dominant harmonic. This method finds the trend and periodic components of a time series as defined by its frequency, amplitude and phase. The addition of several components can be used to describe most of the variability of the original time series. Here, a cross-correlation test was performed between the dominant harmonics of the three time series. These describe the largest percentage of the variability of the original time series and are assumed to be the best choice to determine their interaction in seasonal time scales.

3 Results and discussion

3.1 Climatological maps of NPP

The climatological monthly maps of NPP are shown in the Fig. 3. In January NPP values are below 600 mg C m^{-2} d^{-1}. The values of NPP start to increase in February in the north (27° N) Gulf of Ulloa with values that reach 1000 mg C m^{-2} d^{-1}. By March, NPP increases to 1500 mg C m^{-2} d^{-1} in the northern Gulf. And high values of NPP are present all along the coast of Gulf of Ulloa, with values between 900 mg C m^{-2} d^{-1}. In April the coastal values increase to 1600 mg C m^{-2} d^{-1}. This month is the most productive of the year, in the 5 years considered. In May the NPP starts to diminish, with the coastal values in the range of 900 to 130 mg C m^{-2} d^{-1}. By June, the values in the coastal band are now between 600 and 1250 mg C m^{-2} d^{-1} but now only from middle to northern of the gulf (26–28° N). In July and August there only two small coastal regions can be observed with relatively high values of NPP, between 600 and 900 mg C m^{-2} d^{-1}. From September to December NPP values are very small in all the Gulf of Ulloa, all estimates are below 100 mg C m^{-2} d^{-1}. From these maps a seasonal

OSD
8, 1979–1999, 2011

behavior in the NPP values is evident with maxima in the spring and early summer (from March to June) and with minima from September to December. This is consistent with the upwelling period reported for this region by Zaytsev et al. (2003).

3.2 Climatological maps of SST and currents

The climatological monthly maps of SST are shown in the Fig. 4 (with current field superimposed). In January the SST has values from 14 °C in the north (28° N) to 23 °C in the southern (25° N) Gulf of Ulloa. In February and March the lowest temperatures in the northern coastal band reach ∼15 °C and the maxima decreased to 21 °C. During April and May the coldest water (around 12 °C) is found again in the north but it now extends to the middle of the Gulf of Ulloa (26–28° N) and cover not only the coastal zone but the oceanic water too. This is clearly associated to upwelling processes because the cold water is parallel to the coast throughout the period. By June this behavior is restricted to northern coast with the lowest temperatures close to 15 °C. This appears to be the start of the relaxation of the upwelling because the oceanic water is less cold too. Also in June a mass of coastal warm water (temperatures near to 21 °C) is present in southern Gulf of Ulloa (25–26° N). In July and August the warm water advances poleward to the middle Gulf of Ulloa (26.5° N) not only in the coast but cover all the gulf with higher temperatures of 26 °C, while the coldest water (18–19 °C) is restricted to a small coastal area in the north (27–28° N). By September and October the warmer water covers almost all of the central part of the Gulf of Ulloa (26–27° N) with temperatures of 28 °C. Now the minimum temperature is 20 °C at (27.5° N) and there is no evidence of the colder water associated to upwelling. By November the temperature starts to decrease in northern gulf the SSTs is 18 °C, while at the southern (25° N) SSTs remain around 25 °C. By December the cooling reaches SSTs of 16 °C in a small zone at northern (28° N) and the higher values decrease to 23 °C at southern (25° N). Monthly maps of climatological surface currents are also shown in the Fig. 4, a coastal alongshore equatorward current is present from February to June all over the gulf, the velocity fields are between 0.20 and 0.25 m s^{-1}. During July and August the

OSD
8, 1979–1999, 2011

equatorward flow is not present at the coast but offshore only, the coast remains calm ($<10\,m\,s^{-1}$). The former appears to be related to the southward flow of the California Current. From September to December an eddy dominates the surface current field south of Punta Eugenia (28° N), at the same time there is a poleward flow along this coast (25–27° N). In January this eddy appears to have propagated slightly offshore (between −114 and −116° W) and the equatorward coastal current is lightly present in northern (27–28° N) Gulf of Ulloa. In February the eddy is still offshore at (27–28° N). The maps of SST showed that favorable stronger upwelling conditions (lowest coastal cold water) are present from April to June and less intense in February and March. The stronger upwelling thermal conditions values in this period are coincident with the stronger ($>0.20\,m\,s^{-1}$) equatorward currents (Fig. 4) while the less intense upwelling conditions are coincident with a weak ($<0.20\,m\,s^{-1}$) and oceanic equatorward flow. So, as a result of the upwelling cold waters and coastal equatorward currents are present at the same time, the values of the NPP reach its highest values (Fig. 3). The opposite effect is also true, when warm water is present and the current is poleward the NPP values are the lowest (Fig. 3). This behavior suggest that the locally NPP has a stronger dependence with the combination of local upwelling and the equatorward flow.

3.3 Climatological maps of wind and wind stress curls (WSC)

Climatological monthly maps of WSC and wind vectors are shown in the Fig. 5. The winds are included to show the monthly variability in the region. The winds flow parallel to the coast throughout the year, and particularly so near the coast. The resultant WSC is positive practically all year long, except for a small area in the southern Gulf of Ulloa (25–26° N) that exhibits negative values (downwelling) in February and October. The months with the highest positive values of coastal WSC are March through June (values $>4.5\,m\,s^{-1}\,e^{-7}$ from 25 to 27° N). In July and August the coastal values of WSC lie in the range of 1.5 to $4\,m\,s^{-1}\,e^{-7}$. From September to January values fall below $2\,m\,s^{-1}\,e^{-7}$. In the oceanic dominion the values of WSC are always negative.

OSD
8, 1979–1999, 2011

As indirectly concluded from the SST maps (Fig. 4), the wind and WSC maps (Fig. 5) confirm that local upwelling occurs in the Gulf of Ulloa from March to July (positive WSC). This occurs at the same time when NPP values are highest and also with the presence of a strong equatorward coastal current. It is important to note that even though the wind pattern is upwelling favourable practically throughout the year, high NPP values are present only when the coastal equatorward current is present.

To provide some support to this hypothesis, maps of climatological currents (mean monthly currents from 2003 to 2007) are shown superimposed over NPP climatological monthly maps (same period) in Fig. 6. The circulation pattern from February to June shows a coastal equatorward current in the Gulf of Ulloa. The current is more intense from April to June and during July the current is located offshore. The presence of this equatorward current coincides with the increase of NPP coastal values in March, April and June. The lack of a coastal flow in July and August and the presence of a weak poleward current the rest of the year is associated with a sharp decrease in NPP values. Summarizing, high NPPs occurs during the months of April, May and June when WSC is positive near the coast and coastal temperatures are lowest and the currents flow towards the equator. Lowest NPP's occur near the coast from July to December also with positive WSC but with high coastal temperatures and a poleward coastal current. This suggests that variability of coastal productivity is not only due to local processes such as upwelling but that advection along the coast plays an important role in controlling its seasonal variations.

3.4 Monthly time series

The mean time series of monthly values of the 6 points in Fig. 1 for NPP, WSC and geostrophic alongshore component of the currents (GAC) are shown in Fig. 7 from 2003 to 2007. The NPP (green shaded curve), is present in both the upper (a) and middle panel (b) to compare its seasonal variability with the other variables. Maximum NPP values occur each year in spring-summer and are minimum in the autumn. The most productive year during the period of study is 2003 reaching 750 mg C m^{-2} d^{-1}

OSD
8, 1979–1999, 2011

in the spring. By the end of the summer of 2003 the values decrease to less than 25 mg C $m^{-2} d^{-1}$. In 2004 the highest values of NPP are 450 mg C $m^{-2} d^{-1}$ in late spring and early summer. By 2005, the NPP start to increase above 25 mg C $m^{-2} d^{-1}$ in winter. A secondary high of 400 mg C $m^{-2} d^{-1}$ is present in the early summer but the yearly maximum reaches 450 mg C $m^{-2} d^{-1}$ in the spring. In 2006, from mid-winter to mid-summer the values of NPP lie above 250 mg C $m^{-2} d^{-1}$ with the highest value of 500 mg C $m^{-2} d^{-1}$ in early summer. By 2007, the values of NPP are above 250 mg C $m^{-2} d^{-1}$ all winter and NPP remains high until late spring. In this year the NPP is the lowest in summer for the whole period, but it is the highest in autumn in all five years. The NPP curve for the Gulf of Ulloa is dominated by the seasonal cycle. Some interannual variability is also evident in the high productivity year of 2003.

In Fig. 7a we compare the WSC and NPP curves (upper panel). Positive WSC values occur practically during all 5 years, except for short periods in the winter 2003, autumn 2004, autumn 2007, and late summer 2007. The seasonal variability has two maxima for every year, the first one and with the highest values from 500–1000 m s^{-1} e^{-6} in spring-summer in 2003 and a less intense period in the autumn with values from 250 to 500 m s^{-1} e^{-6}, with the only exception occurring in 2006 when values where slightly negative. In general terms NPP and WSC curves are well correlated: positive values of NPP occur with positive values of WSC. But positive NPP occurs also when WSC values are negative suggesting that the WSC is not the only process enhancing coastal productivity. Vice versa, low values of NPP can occur even if positive WSC is present. In Fig. 7b (middle panel) we compare alongshore currents (GAC) with the NPP curve. GAC values are clearly seasonal. They show negative values (equatorward) from winter to late summer and positive values (poleward) from late summer to autumn. Both the equatorward (–) and the poleward (+) flow reach values of nearly 0.20 m s^{-1}. Whenever the GAC flows equatorward the NPP reach high coastal values (>250 mg C $m^{-2} d^{-1}$). When GAC is close to zero or when it is positive (poleward current) the NPP begin to decrease or presents values below 150 mg C $m^{-2} d^{-1}$. The only exception was the summer of 2003 when even during the summer months, but with a

OSD
8, 1979–1999, 2011

weak poleward flow, NPP values remained high.

Therefore, the GACs are inversely related with NPPs. When GAC values reach a minimum, meaning that a strong equatorward current exists, the NPP reach maximum values. Most of the positive GAC values are accompanied by low values of NPPs and this is consistent with the inhibition of the high productivity when poleward currents arrive carrying warm waters with tropical characteristics. We performed a harmonics analysis of the time series of NPP, GAC and WSC to obtain the dominant harmonic of each time series (Fig. 7c), as explained in the methods. Each harmonic explains 82 %, 76 % and 55 % of the NPP, GAC and WSC variability, respectively. These components explain the seasonal behavior and have a periodicity of 12 months. Only in the case of the WSC time series a second cycle was significant, with the 6-month harmonics capable of explaining an additional 5 % of the variability (not shown). In the case of the NPP and WSC harmonics the yearly maxima occurs almost simultaneously every April–May (cross-correlation coefficient of 0.99 at 0 lag), always preceded (by about one month) by the minima of the GAC indicating equatorward flow (cross-correlation coefficient of 0.97 at −1 lag).

4 Conclusions

Advection plays an important role in modulating the productivity of the west coast of Baja California, at subtropical latitudes. The nutrient-rich waters of the Gulf of Ulloa are due to both the local upwelling and to the equatorward coastal currents that carry nutrient-rich waters from neighboring upwelling areas to the north. The evidence presented over this five-year period is consistent with the seasonal modulation of the NPP by coastal upwelling and coastal currents. Even though the model used to estimate NPP has not been validated by in situ measurements, we believe that the agreement between the forcing, the WSC time series, and the seasonal variation of NPP validate the observed seasonal and interannual signal. There is also evidence that mesoscale process plays a part in the redistribution of coastal properties but the subject is beyond

OSD
8, 1979–1999, 2011

the scope of the present study. The effects of interannual ENSO-like phenomena are also present in our data and they will be the subject of future work.

Acknowledgements. Products from ESA's ERS-1 and ERS-2 data, CNES/NASA TOPEX/POSEIDON data and CLS "SLA" were used. The altimeter products were produced by the CLS Space Oceanography Division as part of the Environment and Climate EU ENACT Project (EVK2-CT2001-00117) and with support from CNES. QuickSCAT level 3 daily data is freely available at the web site of the Jet Propulsion Laboratory. MODIS level 3 data are freely available at the web site of OceanColor. HYCOM simulations were performed as part of the Office of Naval Research project Eddy Resolving Global Ocean Prediction Including Tides using challenge and non challenge time from the US Department of Defense (DOD) High Performance Computing Modernization Office on Cray XT5 and IBM P6 computers at the Navy DOD Supercomputing Resource Center, Stennis Space Center. Funding for this project came from the Consejo Nacional de Ciencia y Tecnología (CONACYT-México), project 32500-T. EGR, ATC and GGC are grant holders of the Sistema Nacional de Investigadores (CONACYT). Partial funding was also provided by the División de Oceanología of CICESE and by CICESE Unidad La Paz.

References

Bakun, A. and Nelson, C. S.: Climatology of upwelling related processes off Baja California., CALCOFI Report, 19, 107–127, 1977. 1981

Behrenfeld, M. J. and Falkowski, P. G.: Photosynthetic rates derived from satellite based chlorophyll concentration, Limnol. Oceanogr., 42, 1–20, 1997. 1982

Bleck, R.: An oceanic general circulation model framed in hybrid isopycnic-cartesian coordinates, Ocean Model, pp. 55–88, doi:10.1016/S1463-5003(01)00012-9, 2002. 1983

Bliss, C. I.: Periodic Regression in Biology and Climatology, New Haven, Connecticut Agricultural Experiment Station, Bulletin, p. 55, 1958. 1985

Brink, K. H. and Cowles, T. J.: The Coastal Transition Zone Program, J. Geophys. Res., 96, 14637–14647, doi:10.1029/91JC01206, 1991. 1981

Gill, A. E.: Atmosphere-Ocean Dynamics, Academic Press, International, 1982. 1984

Haynes, R., Barton, E. D., and Pilling, I.: Development, Persistence, and Variability of Upwelling

OSD

8, 1979–1999, 2011

Filaments off the Atlantic Coast of the Iberian Peninsula, J. Geophys. Res., 98, 22681–22692, doi:10.1029/93JC02016, 1993. 1981
Hickey, B. M.: The California current system–hypotheses and facts, Progress In Oceanography, 8, 191–279, doi:10.1016/0079-6611(79)90002-8, http://www.sciencedirect.com/science/article/B6V7B-48CFVK2-3/2/ed897f4bd8b15e53c4f9a363c37dbe23, 1979. 1981
Huyer, A.: Coastal upwelling in the California current system, Progress In Oceanography, 12, 259–284, doi:10.1016/0079-6611(83)90010-1, http://www.sciencedirect.com/science/article/B6V7B-48BDPS0-N/2/a87e49c2bc3ded3bf8151bda442ea95a, 1983. 1981
Levitus, S. and Gelfeld, R.: Key to Oceanography Records Documentation, No. 18., chap. NODC inventory of physical oceanography profiles., US Government Printing Office, Washington, D.C., 1992. 1984
Lluch-Belda, D.: BAC's: Centros de Actividad Biológica del Pacífico Mexicano, chap. Centros de Actividad Biológica en la costa de Baja California, pp. 49–64, CIBNOR CONACyT, 1999. 1980, 1981
Lynn, R. J.: Seasonal variation of temperature and salinity at 10 meters in the California current, CalCOFI Report, 11, 157–186, 1967. 1981
Lynn, R. J. and Simpson, J. J.: The California Current System: The Seasonal Variability of its Physical Characteristics, J. Geophys. Res., 92, 12947–12966, doi:10.1029/JC092iC12p12947, 1987. 1981
Morel, A. and Berthon, J.-F.: Surface Pigments, Algal Biomass Profiles, and Potential Production of the Euphotic Layer: Relationships Reinvestigated in View of Remote-Sensing Applications, Limnol. Oceanogr., 34, 1545–1562, http://www.jstor.org/stable/2837038, 1989. 1983
Nelson, C. S.: Wind stress and wind stress curl over the California current, Tech Report, NMFS-NOAA, pp. 1–87, 1977. 1981
Strub, P. T. and James, C.: The 1997–1998 oceanic El Niño signal along the southeast and northeast Pacific boundaries–an altimetric view, Progress In Oceanography, 54, 439–458, doi:10.1016/S0079-6611(02)00063-0, http://www.sciencedirect.com/science/article/pii/S0079661102000630, 2002. 1984
Zaytsev, O., Cervantes-Duarte, R., Montante, O., and Gallegos-Garcia, A.: Coastal Upwelling Activity on the Pacific Shelf of the Baja California Peninsula, J. Oceanogr., 59, 489–502, doi:10.1023/A:1025544700632, 2003. 1981, 1986

OSD
8, 1979–1999, 2011

Fig. 1. The Gulf of Ulloa. The 6 grey filled circle are the sites where we sampled the NPP, currents and winds to generate mean time series for the region. The thin lines indicate the isobaths to 200 and 1000 m.

OSD
8, 1979–1999, 2011

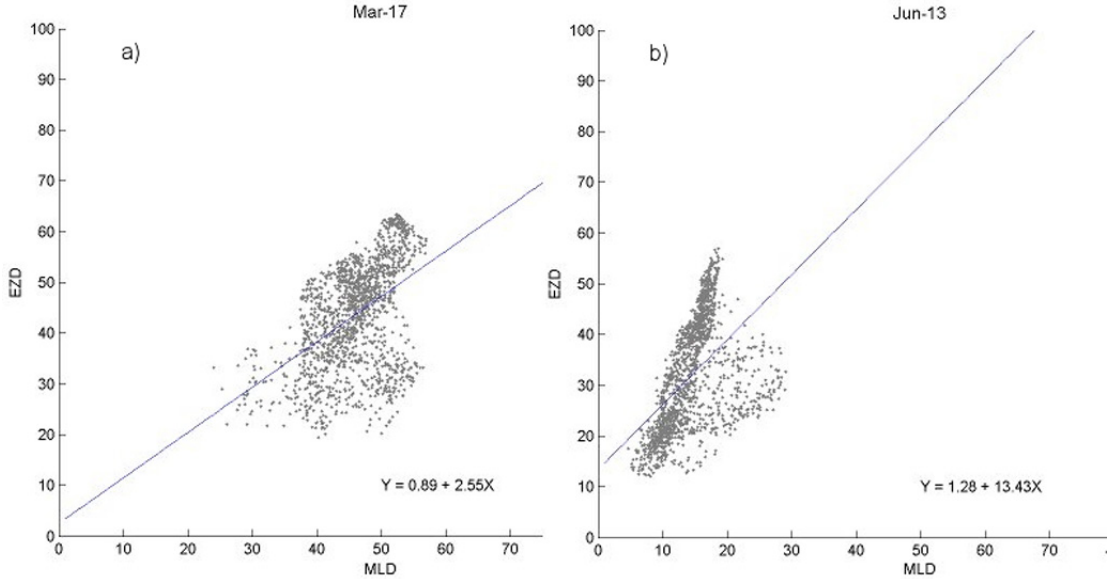

Fig. 2. Relationship between Z_{eu} and MLD during upwelling season. Panel **(a)** at season begin in March and panel **(b)** season later in June.

OSD
8, 1979–1999, 2011

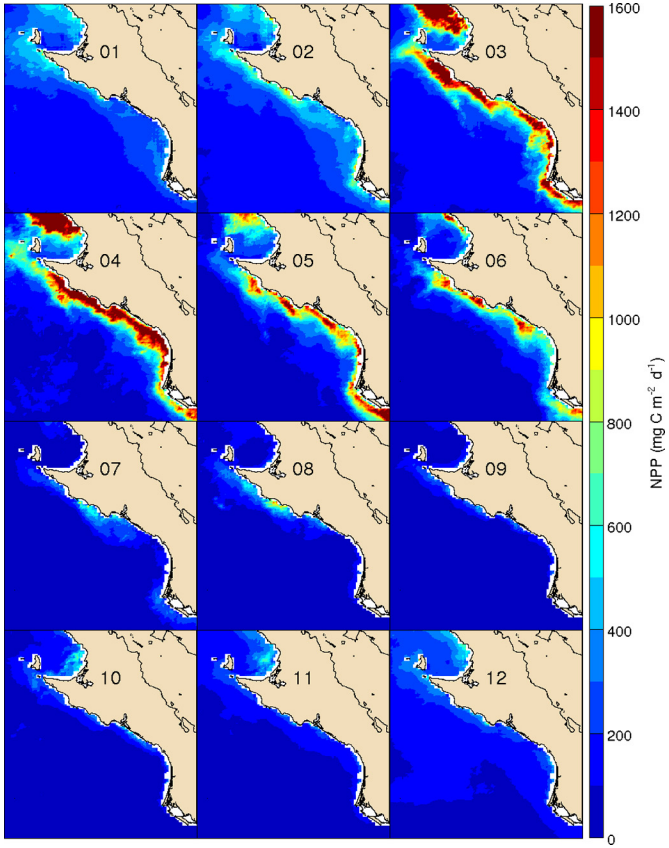

Fig. 3. Monthly climatology of NPP for the period 2003 to 2007. Numbers in each panel indicate the month of the year.

OSD
8, 1979–1999, 2011

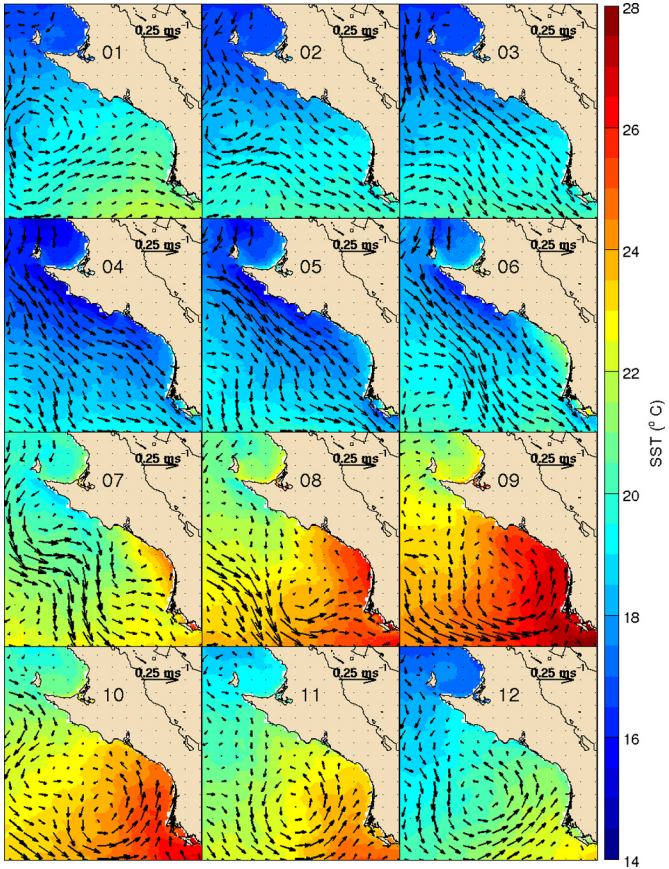

Fig. 4. Maps of monthly mean sea surfer temperature (SST) and geostrophic currents for the period 2003–2007. Numbers in each panel indicate the month of the year.

OSD
8, 1979–1999, 2011

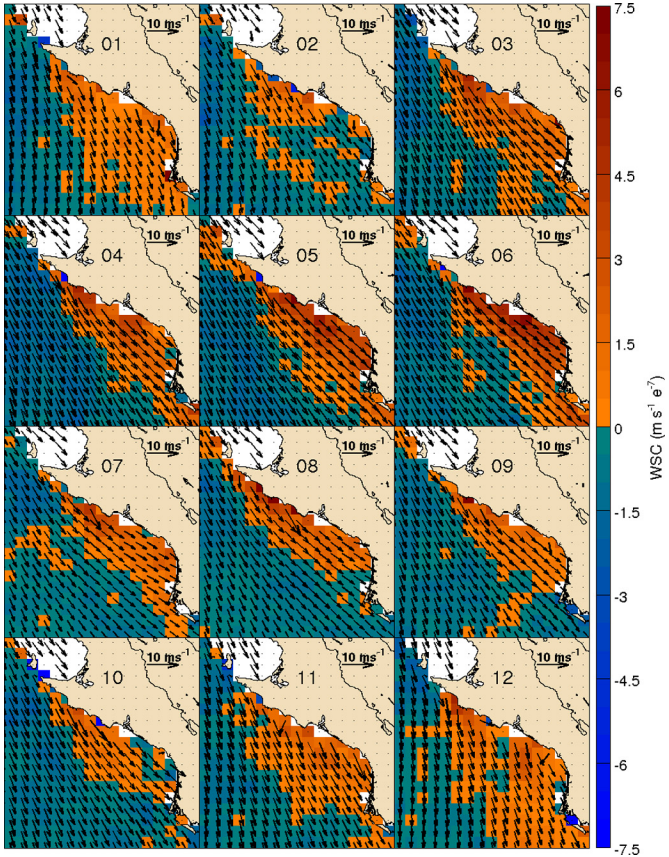

Fig. 5. Maps of monthly mean of wind vectors and wind of stress curl (WSC) for period 2003–2007. Numbers in each panel indicate the month of the year.

OSD
8, 1979–1999, 2011

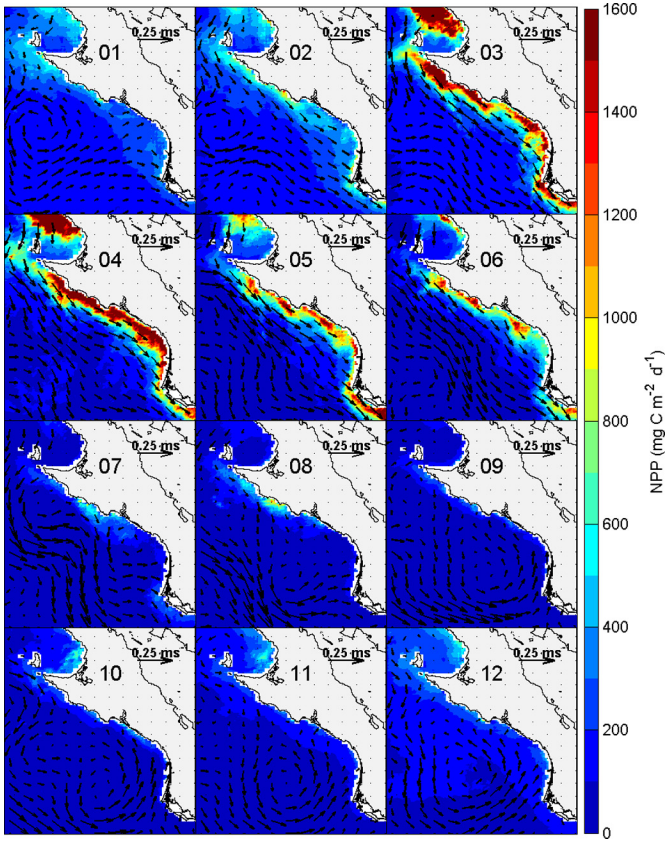

Fig. 6. Maps of monthly net primary productivity (NPP) and geostrophic currents for period 2003–2007. Numbers in each panel indicate the month of the year.

OSD
8, 1979–1999, 2011

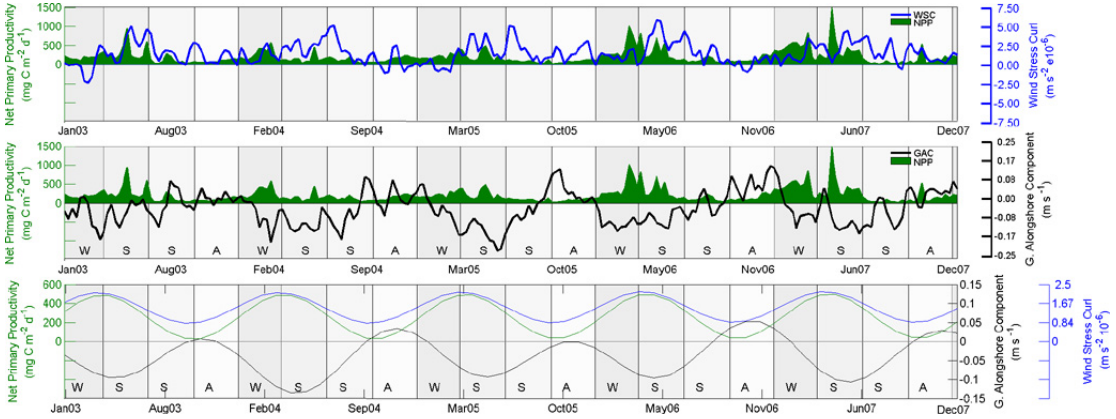

Fig. 7. **(a)** Time series of net primary productivity (NPP, green shaded) with wind stress curl (WSC, blue solid line) for period 2003–2007. **(b)** Time series of NPP (green shaded) with geostrophic alongshore component (GAC, black solid line) for period 2003–2007. **(c)** Dominant harmonics of the time series of NPP (green line), WSC (blue line) and GAC (black line).

OSD
8, 1979–1999, 2011